Local Geographic Atrophy Growth Rates Not Influenced by Close Proximity to Non-Exudative Type 1 Macular Neovascularization

Omer Trivizki,[1] Eric M. Moult,[2] Liang Wang,[1] Prashanth Iyer,[1] Yingying Shi,[1] Giovanni Gregori,[1] William Feuer,[1] James G. Fujimoto,[2] and Philip J. Rosenfeld[1]

[1]Department of Ophthalmology, Bascom Palmer Eye Institute, University of Miami Miller School of Medicine, Miami, Florida, United States
[2]Department of Electrical Engineering and Computer Science, Research Laboratory of Electronics, Massachusetts Institute of Technology, Cambridge, Massachusetts, United States

Correspondence: Philip J. Rosenfeld, Bascom Palmer Eye Institute, 900 NW 17th street, Miami, FL 33136, USA;
prosenfeld@miami.edu.

Received: August 20, 2021
Accepted: November 17, 2021
Published: January 14, 2022

Citation: Trivizki O, Moult EM, Wang L, et al. Local geographic atrophy growth rates not influenced by close proximity to non-exudative type 1 macular neovascularization. *Invest Ophthalmol Vis Sci.* 2022;63(1):20. https://doi.org/10.1167/iovs.63.1.20

Purpose. The local growth rates of geographic atrophy (GA) adjacent to non-exudative type 1 macular neovascularization (MNV) were investigated to determine if MNV influenced GA growth.

Methods. Eyes with GA and non-exudative type 1 MNV were followed for at least 1 year. Both GA and the MNV were imaged and measured using swept-source optical coherence tomography angiography (SS-OCTA) scans. Pearson correlations were computed between local growth rates of GA, which were estimated using a biophysical GA growth model, and local distances-to-MNV. Corresponding P values for the null hypothesis of no Pearson correlation were computed using a Monte Carlo approach that adjusts for spatial autocorrelations.

Results. Nine eyes were included in this study. There were positive correlations (Pearson's $r > 0$) between distance-to-MNV and local GA growth in eight (89%) of the eyes; however, in all but one eye (11%), correlations were relatively weak and statistically nonsignificant after Bonferroni correction (corrected $P > 0.05$).

Conclusions. SS-OCTA imaging combined with GA growth modeling and spatial statistical analysis enabled quantitative assessment of correlations between local GA growth rates and local distances-to-MNV. Our results are not consistent with non-exudative type 1 MNV having a strong inhibitory effect on local GA growth rates.

Keywords: geographic atrophy (GA), optical coherence tomography angiography (OCTA), non-exudative type 1, macular neovascularization (MNV), growth rate

Age-related macular degeneration (AMD), the leading cause of irreversible blindness worldwide, is a degenerative disease of the macula, often leading to progressive vision loss. AMD has early and late stages, with visual impairment occurring in the latter.[1] Late stage AMD is characterized either by the formation of macular neovascularization (MNV) or progressive atrophy of the RPE, choriocapillaris, and photoreceptor layers, which is termed geographic atrophy (GA) or complete retinal pigment epithelium and outer retinal atrophy (cRORA).[2,3]

Based on their clinical appearances, GA and MNV are frequently considered to be distinct AMD subtypes.[4] However, both are associated with common variants in the CFH and ARMS2 genes,[5–7] co-exist with drusen and reticular pseudodrusen, and occur simultaneously at a frequency that is probably underestimated, all of which suggest a possible overlap of their pathological mechanisms.[8,9] Indeed, histopathological studies have reported the co-existence of GA and MNV in the same eye, which may not always be evident clinically. In a study of 46 eyes with the clinical diagnosis of GA, Sarks et al. found that 15 eyes had subclinical MNV on histology.[10] In two other histopathological studies, Green et al. found that 22 eyes of 63 patients with clinical bilateral MNV also had areas of RPE atrophy on histology,[11] and 86 of 760 eyes with a pre-mortem diagnosis of AMD demonstrated both MNV and RPE atrophy histologically.[12] Hypothetically, the formation of type 1 MNV beneath the RPE may provide nutritional support for the RPE and photoreceptors and slow the formation of GA by recapitulating the choriocapillaris, as first proposed by Grossniklaus et al.[13]

More recently, using optical coherence tomography angiography (OCTA), Pfau et al. found that the progression of RPE atrophy was markedly reduced in areas adjacent to type 1 MNV.[14] Thus, the reduced GA growth rate observed by Pfau et al. could plausibly be attributed to protective effects of the MNV. However, Pfau et al. did not distinguish between GA adjacent to MNV and GA embedded within MNV. Because MNV can evolve into macular atrophy that may be indistinguishable from GA, and because

controversy persists whether injections of vascular endothelial growth factor (VEGF) inhibitors may influence the formation of GA,[12,15,16] there may be a difference between the growth of GA embedded within the MNV versus growth of GA adjacent to untreated non-exudative MNV.

In this current study, we investigated whether non-exudative type 1 MNV was associated with reduced local GA growth rates. We decided to focus on the non-exudative form of type 1 MNV because it is plausible that both exudation and its subsequent treatment could affect any potential protection afforded by the MNV. The approach of this study was to test the hypothesis that the distance to the MNV is Pearson correlated with local GA growth rates, and this hypothesis was tested by using a combination of swept-source optical coherence tomography angiography (SS-OCTA) imaging, GA growth modeling, and spatial statistical methods.

Methods

Patients were enrolled into an ongoing institutional review board-approved prospective SS-OCTA imaging study that was approved by the Institutional Review Board (IRB) of the University of Miami Miller School of Medicine and that followed the tenets of the Declaration of Helsinki and the Health Insurance Portability and Accountability Act of 1996 regulations. Patients selected for this study were diagnosed with non-exudative type 1 MNV using SS-OCTA imaging. as previously described.[17–20] The type 1 MNV was adjacent to an area of GA $\geq$2.54 mm^2 (one disc area), and for multifocal lesions, the MNV had to be adjacent to an area of GA with an area $\geq$1.25 mm^2; and all GA foci and MNV had to also be fully contained within the 6 mm $\times$ 6 mm field-of-view at all visits. Additionally, eyes were excluded if the GA was continuous with peripapillary atrophy. None of the study eyes had been previously treated. Eyes with atrophy embedded within an area of type 1 MNV were excluded, and MNV surrounded by atrophy were excluded. The interval between the baseline visit (visit 1) and the follow-up visit (visit 2) was approximately 1 year for all included eyes.

SS-OCTA (PLEX Elite 9000; Carl Zeiss Meditec, Dublin, CA, USA) images were acquired over 6 mm $\times$ 6 mm fovea-centered fields-of-view. Baseline and follow-up GA margins were manually traced by two experienced readers (authors O.T. and L.W.) using en face sub-RPE OCT slabs, which were formed by sum projection of the OCT volume in a slab located 64 to 400 µm below Bruch's membrane. Consensus grading was achieved between graders, and whenever a consensus could not be reached, the senior grader (author P.J.R.) adjudicated the disagreement and a final grading was achieved. GA measurements using en face sub-RPE OCT slabs have been shown to correlate well with those from fundus autofluorescence (FAF).[21] The general workflow of the imaging processing is shown in Figure 1. The GA area measurements from the sub-RPE OCT slabs at the baseline and follow-up visits were spatially registered using second-order polynomial transformations estimated from manually selected fiducial points, as described in Moult et al. Registration accuracy was confirmed by overlaying the registered en face retinal OCTA images. MNV lesions at the baseline visit were manually outlined on en face SS-OCTA images formed by projecting the OCTA volumes between the RPE and Bruch's membrane, and were reviewed by two experienced readers (authors O.T. and L.W.). Any disagreements were adjudicated by a senior grader (author P.J.R.).

Figure 2 provides a graphical explanation of how the local GA growth rates, the local distances-to-MNV, and their correlations were computed. Local GA growth trajectories (see Fig. 2C), which traces the path along which the margin

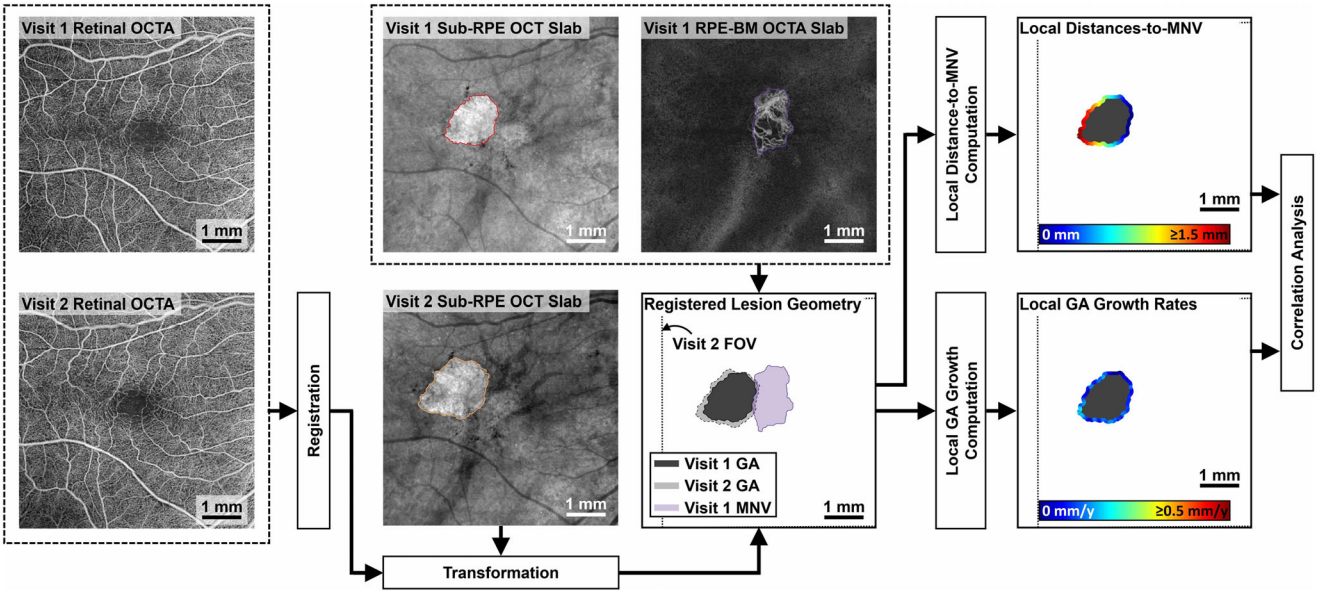

Figure 1. Overview of the methodology used to assess correlations between local geographic atrophy (GA) growth rates and local distances to the macular neovascularization (MNV). Retinal swept-source optical coherence angiography (SS-OCTA) images from visit 1 and visit 2 were registered using fiducials manually placed at corresponding retinal positions (at retinal vessel bifurcations).[22] The estimated registration was then used to transform the visit 2 GA tracings into the visit 1 coordinate frame, allowing the visit 2 GA tracing to be overlaid with the visit 1 MNV and GA tracings. The registered lesion geometries were then used to compute the local GA growth rates (using the visit 1 and visit 2 GA geometries) and the local distances-to-MNV (using the visit 1 GA and visit 1 MNV geometries) at each visit 1 GA margin position. A correlation analysis was then performed on these paired measurements.

Investigative Ophthalmology & Visual Science

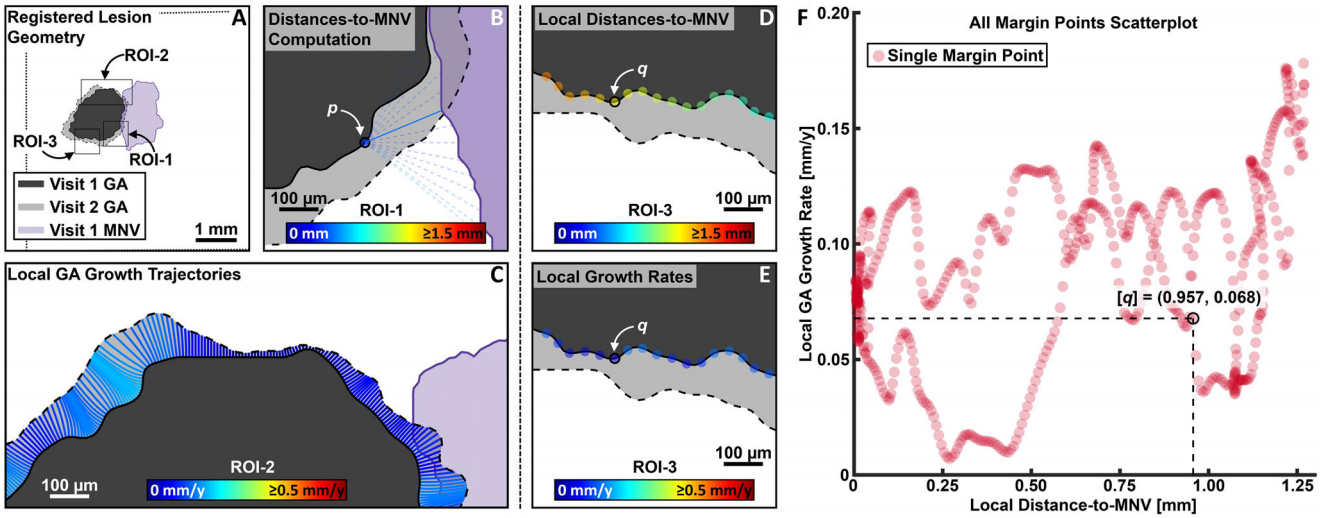

Figure 2. Graphical explanation of how the local geographic atrophy (GA) growth rates, the local distances to the macular neovascularization (MNV), and their correlations were computed. (**A**) Registered lesion geometry, as in Figure 1, with three regions-of-interest (ROIs) overlaid. (**B**) Illustration of the distance-to-MNV computation for a margin point, *p*, located in ROI 1. (**C**) Local GA growth trajectories, which are used to compute local GA growth rates, shown for ROI 2. (**D, E**) Illustration of the paired local GA growth rate and local distance-to-MNV measurements for ROI 3. A particular margin point, *q*, is noted. (**F**) Scatterplot of local GA growth rates versus local distances-to-MNV, where each red marker corresponds to a margin point (note that the red color is for visibility only and is not associated with the color bars of previous panels).

is estimated to grow,[22] were computed as described in Moult et al.[23] Note that, for the case of a circular unifocal lesion growing at the same rate along the entire margin, growth trajectories correspond to radial vectors, perpendicular to the lesion margin. When lesions have more complex geometries and/or growth patterns, growth trajectories become commensurately complex. For each sampled visit 1 margin position, separated by 6 µm in arclength, local GA growth rates were computed as the length of the corresponding growth trajectory divided by the inter-visit time (see Fig. 2E). The corresponding distance-to-MNV was computed as the (Euclidean) distance to the closest point on the MNV border. Conceptually, for a point *p* (see Fig. 2B), the distance-to-MNV can be understood as the length of the shortest line (drawn solid) connecting *p* to any point on the MNV margin (other, longer lines, which connect *p* to different MNV margin points, are drawn dashed). This process is repeated for each of the visit 1 margin positions at which the local GA growth rate was measured (see Fig. 2D). Together, the local GA growth rate and distance-to-MNV analyses yield a set of paired measurements taken at each sampled visit 1 GA margin position (see Figs. 2D, 2E). These paired measurements can then be displayed on a scatterplot with x-coordinates corresponding to distances-to-MNV and y-coordinates corresponding to local GA growth rates (see Fig. 2F). Each marker in the scatterplot corresponds to a particular position along the visit 1 margin. For example, the point, *q* (see Figs. 2D, 2E), can be located on the scatterplot using its x-coordinate (its distance-to-MNV) and its y-coordinate (its local GA growth rate), as depicted. If there were a positive (linear) correlation between local GA growth rates and local distances-to-MNV, we would expect the scatterplot points to lie along an upward sloped line.

The association between these paired measurements was assessed using Pearson's correlation (see Fig. 2F) within two regions-of-interest, one comprised of all visit 1 GA margin points ("all distances analysis") and another comprised of only those visit 1 GA margin points having a distance less than 1 mm from the MNV border ("1-mm analysis"). This two-fold analysis was performed to investigate the possibility that any potentially protective effects of the MNV are constrained within a "neighborhood of influence" (see Discussion). Corresponding *P* values for the null hypothesis of no Pearson correlation were estimated using a Monte Carlo permutation scheme that incorporates the effects of spatial autocorrelation.[23,24] The importance of compensating for spatial autocorrelations is detailed in Moult et al.[23]

Results

Nine eyes from nine patients were included in the study. The global square-root-of-area growth rates in 7 (78%) of the eyes were lower than the literature-reported average of ~0.3 mm/year for GA eyes without MNV,[25,26] although this could be a result of the inclusion criteria of this study, which excluded eyes with total baseline lesion areas less than one disc area (2.54 mm^2), eyes with GA embedded within the MNV, and MNV surrounded by GA (Table). The average lesion area at visit 1 was 3.05 ± 2.76 mm^2. For the all distances analysis and the 1-mm analysis, there were positive correlations (Pearson's $r > 0$) between distance-to-MNV and local GA growth in 8 (89%) and 6 (67%) of the eyes, respectively; however, in all but 1 eye (11%), correlations were relatively weak and statistically nonsignificant after Bonferroni correction (corrected $P > 0.05$). Figures 3, 4, and 5 summarize the GA and MNV tracings, local GA growth trajectories, and scatterplots and boxplots of local GA growth rates versus distances-to-MNV. Considering the scatterplots, only case 9 (see Fig. 5C) shows a qualitative association between local distance-to-MNV and local GA growth rate, agreeing with the statistical assessment (see the Table). It is also interesting to note that the positive correlation of case 1, which has a statistically significant pre-correction *P* value ($P < 0.05$), is likely to be, in part,

Investigative Ophthalmology & Visual Science

Table. Patient Characteristics, Baseline Lesion Areas, Global Growth Rates, and Local Correlations

								All Distances		<1 mm	
Case	Age	Gender	Smoking Status	Fellow Eye Status	Follow-Up Time, mo	Visit 1 GA Area, mm^2	Global Growth Rate,* mm/y	Pearson's *r*	*P* Value	Pearson's *r*	*P* Value
1	85	M	AS	GA	13.1	2.43	0.09	0.49	0.024	0.39	0.053
2	71	M	FS	Wet	11.7	1.6	0.11	0.04	0.829	−0.25	0.190
3	83	M	AS	Wet	12.1	8.77	0.12	0.10	0.525	−0.49	0.063
4	95	M	NS	Wet	12.2	5.49	0.12	−0.03	0.804	−0.10	0.497
5	80	F	NS	Wet	11.5	5.67	0.14	0.04	0.807	0.34	0.055
6	95	M	NS	GA	12.9	0.16	0.16	0.37	0.110	0.29	0.324
7	92	M	FS	Int.	11.7	1.83	0.17	0.23	0.511	0.20	0.540
8	92	F	NS	GA	12.0	1.26	0.36	0.02	0.955	0.49	0.304
9	90	F	NS	GA	12.0	0.32	0.42	0.71	0.002	†	†

M, male; F, female; AS, active smoker; FS, former smoker; NS, non-smoker; Int., intermediate AMD.
* Measured using the global square-root-of-area-growth rate.
† For case 9, all visit 1 GA margin points were <1 mm for the MNV border, and so the all distance and 1-mm distance analyses were the same.

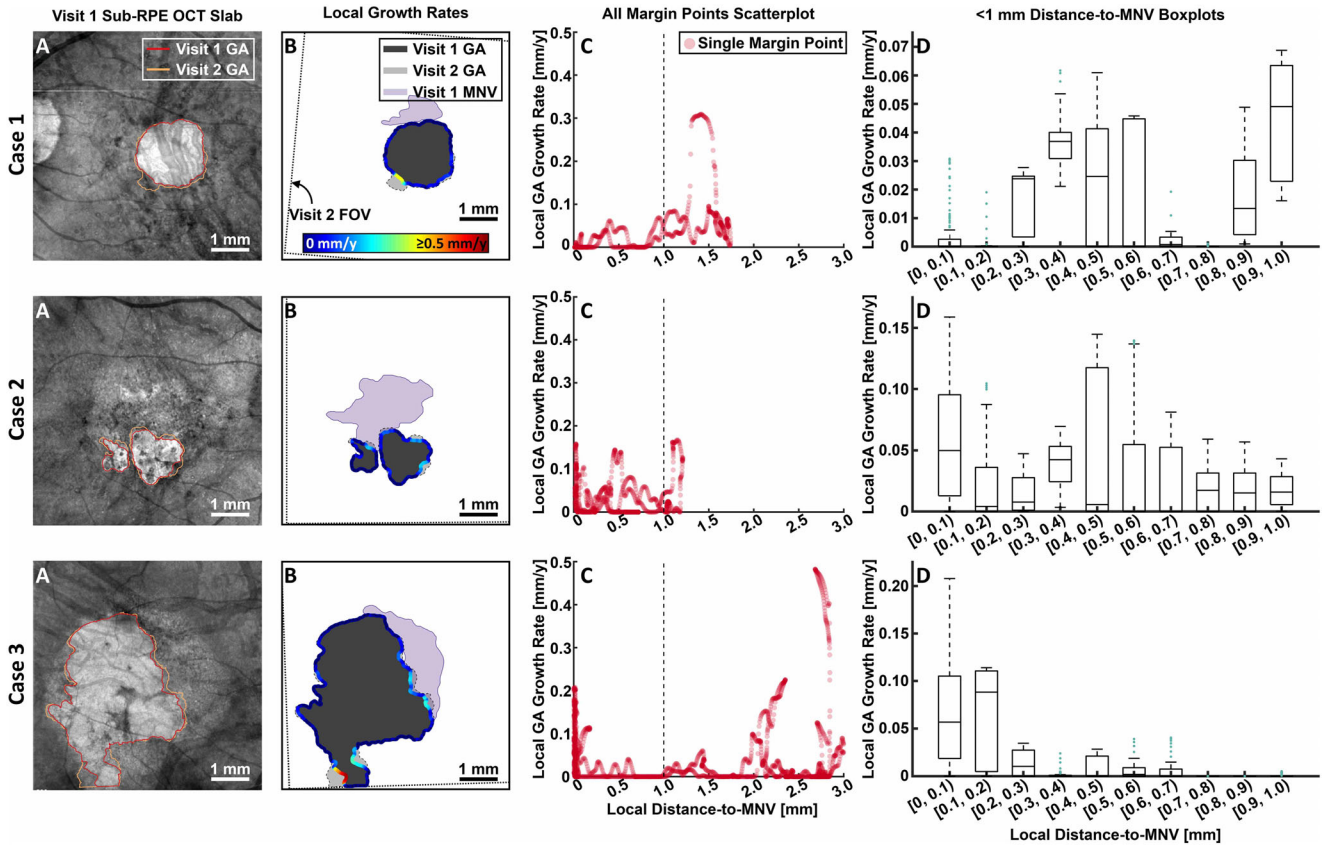

Figure 3. Analysis of case 1 (row 1), case 2 (row 2), and case 3 (row 3). (**A**) Visit 1 sub-RPE OCT slab with the visit 1 and visit 2 margins of the geographic atrophy (GA) overlaid. (**B**) Local GA growth rates displayed along the visit 1 GA margin (see color bar). (**C**) Scatterplot of local GA growth rates versus local distances to the macular neovascularization (MNV). The vertical dashed line corresponds to the 1 mm distance-to-MNV. (**D**) Boxplots, in 100 µm distance-to-MNV intervals, of the local GA growth rates within 1 mm from the MNV. Outliers are indicated by teal markers.

a consequence of a small set of fast-growing margin points positioned opposite the MNV position. While influencing the correlation analysis due to their high leverage, it is unlikely that these points reflect a meaningful physiological correlation between local distance-to-MNV and local GA growth rates.

Discussion

GA and MNV are frequently thought to be distinct subtypes of late AMD. Although their diverse clinical manifestations support this distinction, their co-existence appears to suggest that their pathological cascades may overlap.[4]

Investigative Ophthalmology & Visual Science

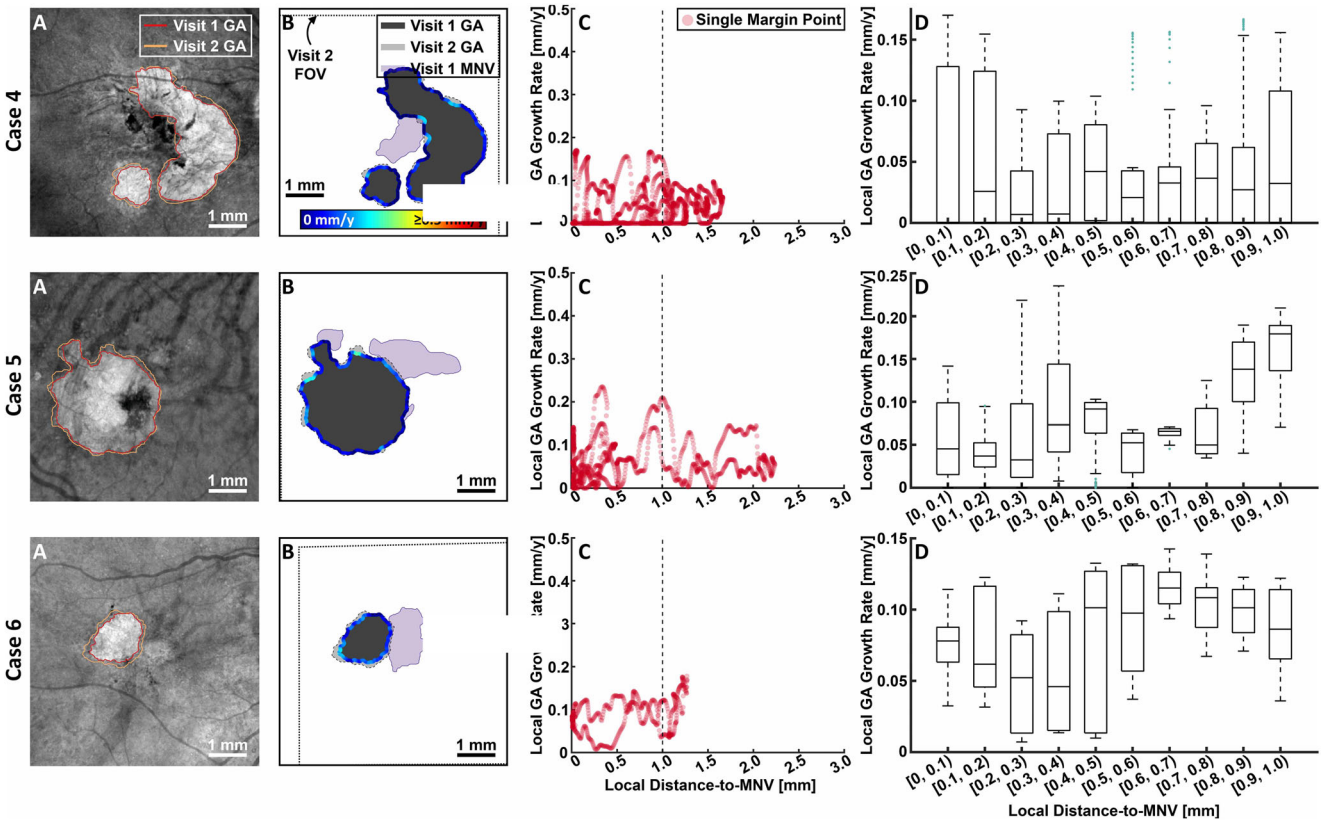

Figure 4. Analysis of case 4 (row 1), case 5 (row 2), and case 6 (row 3). (**A**) Visit 1 sub-RPE OCT slab with the visit 1 and visit 2 margins of the geographic atrophy (GA) overlaid. (**B**) Local GA growth rates displayed along the visit 1 GA margin (see color bar). (**C**) Scatterplot of local GA growth rates versus local distances to the macular neovascularization (MNV). The vertical dashed line corresponds to the 1 mm distance-to-MNV. (**D**) Boxplots, in 100 µm distance-to-MNV intervals, of the local GA growth rates within 1 mm from the MNV. Outliers are indicated by teal markers.

Our current study provides a quantitative assessment of the changes in local GA growth rates as a function of distance-to-MNV. In all but one eye (case 9), the estimated local correlations were weak and statistically nonsignificant (adjusted $P > 0.05$). Moreover, although there was a preponderance of positive correlations in the all distances analysis, this proportion decreased in the 1-mm analysis, which is likely more reflective of a physiologically plausible neighborhood of influence for any MNV-associated growth inhibition. Finally, qualitative inspection of the scatterplots and boxplots were, in general, not supportive of a strong inhibitory effect of MNV near the GA border.

It is interesting to compare our results to those of Pfau et al., who, using local-scale mixed-effects logistic regression, found that the presence of both treatment-naïve non-exudative and exudative type 1 MNV was associated with reduced odds of RPE atrophic progression (odds ratio [95% confidence interval {CI}] of 0.21 [0.19, 0.24], $P < 0.001$). While utilizing different metrics (odds ratios versus correlations), the associations of our study appear to be less pronounced than those of Pfau et al. However, when comparing results, there are important methodological differences to consider. First, our study uses a GA growth model to estimate local GA growth rates, whereas the study by Pfau et al. used Euclidean distances. As discussed in Moult et al.,[22] for non-convex lesion geometries, Euclidean distance computations can result in nonphysical measurements (e.g. growth trajectories passing through regions of non-atrophy). Nevertheless, for smaller growths, we would expect the two approaches to yield similar measurements. Second, the statistical analysis of our approach adjusts for spatial autocorrelations between the distance-to-MNV and local GA growth rate measurements, which is not the case for the pixel-level analysis of Pfau et al. In particular, spatial autocorrelations arise in the analysis of Pfau et al. because if a pixel X develops atrophy, it is more likely that a pixel Y close to X will also develop atrophy than it is that a pixel Z far from X will develop atrophy, even if Y and Z are equidistant from the lesion margin (a covariate included in their model). The presence of autocorrelations is potentially problematic as it reduces the effective sample size, and therefore leads to artificially low P values (i.e. increased type I errors). For example, the effect of autocorrelation adjustment in our analysis can be seen in the assessment of case 8, where there is a larger P value for the 1-mm analysis compared to the all distance analysis, despite Pearson's r being larger for the former. Third, the study by Pfau et al. modeled local MNV presence as a binary variable (i.e. presence or absence of MNV at a given pixel), whereas we modeled MNV presence as a continuous variable (i.e. distance-to-MNV). Fourth, by using mixed-effects modeling, Pfau et al. included the eccentricity and angle (i.e. superior, inferior, nasal, and temporal) as covariates, which were not modeled in our analysis. Inclusion of eccentricity, in particular, may be relevant, as studies have reported variations in average GA growth rates as a function of eccentricity.[27–32] However,

Investigative Ophthalmology & Visual Science

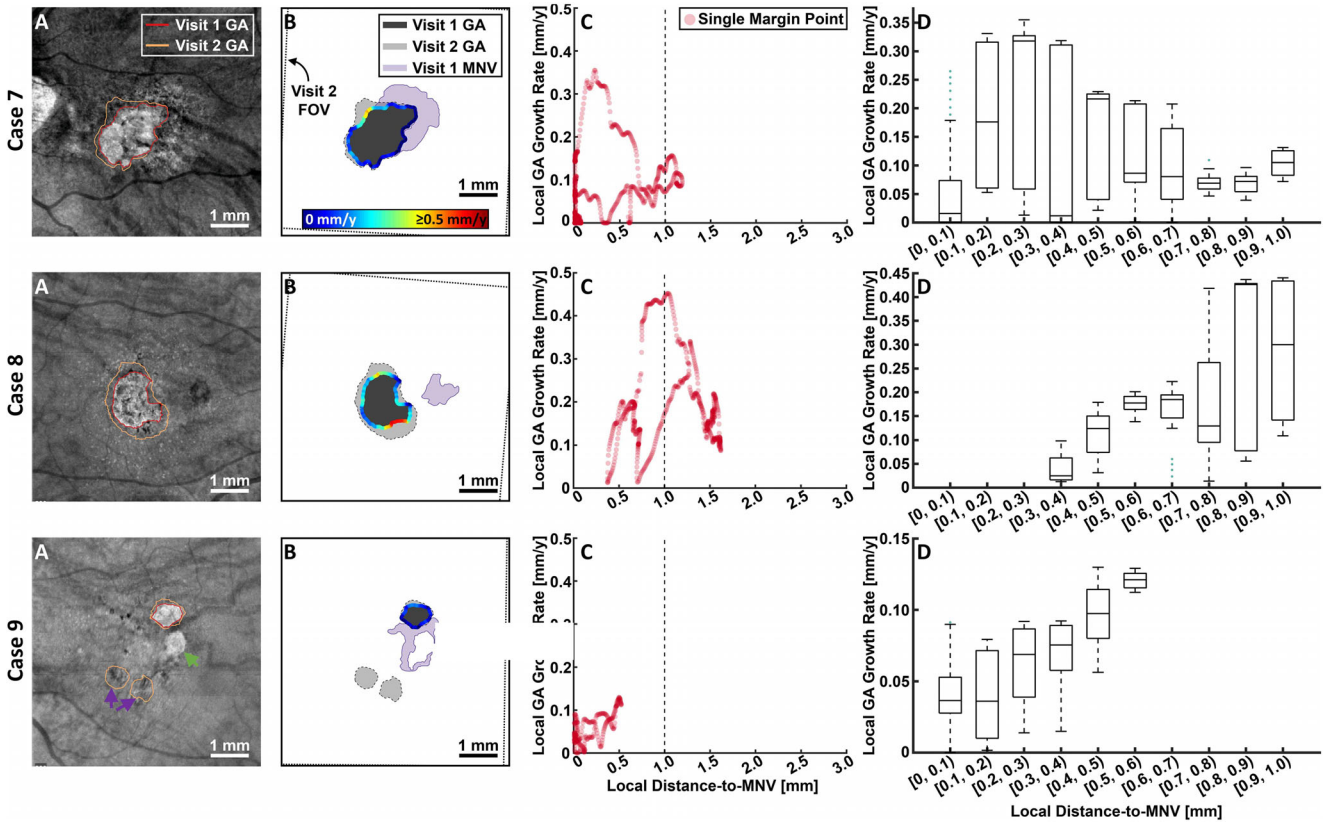

Figure 5. Analysis of case 4 (row 1), case 5 (row 2), and case 6 (row 3). (**A**) Visit 1 sub-RPE OCT slab with the visit 1 and visit 2 margins of the geographic atrophy (GA) overlaid. The green arrow in panel **A** of case 9 points to a region of OCT hyper-transmission that was excluded from the GA tracing because it is surrounded by the MNV lesion (see panel **B**, same row). The purple arrows in panel **A** of case 9 points to two newly appearing GA foci, which were not included in the analysis. (**B**) Local GA growth rates displayed along the visit 1 GA margin (see color bar). (**C**) Scatterplot of local GA growth rates versus local distances to the macular neovascularization (MNV). The vertical dashed line corresponds to the 1 mm distance-to-MNV. (**D**) Boxplots, in 100 µm distance-to-MNV intervals, of the local GA growth rates within 1 mm from the MNV. Outliers are indicated by teal markers.

these studies investigated dependencies of GA growth rates as a function of eccentricity pooled over many eyes, rather than intra-eye dependencies, which are the only type of dependency relevant to the present study. Nevertheless, to investigate this potential confounder, we generated scatterplots (Fig. 6) of the local GA growth rates versus the local distance to the fovea center, estimated as the center of the FAZ as traced on OCTA. Examination of these scatterplots shows no evidence of a confounding intra-eye correlation between local GA growth rates and eccentricity. Fifth, Pfau et al. included embedded GA cases, which we excluded in our analysis given the possibility that atrophy in the center of MNV has different etiology and character as compared to GA that develops independently of MNV.

Although the exact sequence of events that leads to RPE atrophy is unknown, it is clear that there is significant deterioration of both the choriocapillaris and Bruch's membrane in addition to deterioration of the RPE.[2] Quantitative OCTA-based analyses have been used to study associations between GA growth rates and choriocapillaris impairment.[23] These data, which showed increasing (global) GA growth rates with increased CC impairment, support current considerations of GA pathogenesis. The physiological development and location of type 1 MNV has been thought to have a protective effect on adjacent GA progression,[3] with the angiogenic process contributing to a decrease in GA growth rates.[5] It has been proposed that the MNV could be an attempt to recapitulate the choriocapillaris under the RPE, thus preserving the RPE and preventing the growth of GA. However, our results appear to show that, if MNV is indeed such an attempt, it is an unsuccessful one, at least as it concerns the slowing of local GA growth. Perhaps, GA is less likely to form in areas where non-exudative MNV is present, but that question is different to the one addressed in the present study.

Our study has several limitations that are important to consider. First, our small cohort size makes generalization difficult; however, if GA does have an impact of local GA growth, it appears not to be very strong. Second, our local GA growth rate measurements were estimated using our atrophy-front growth model,[22] which, as all models, incompletely captures true GA growth dynamics. Nevertheless, in addition to having some basic physiologic plausibility,[22,23] our model has advantages over the Euclidean-based approach, which can produce nonphysical growth trajectories. Third, we assessed the associations between local GA growth rates and distances-to-MNV via Pearson's correlation, which is most often used for quantifying linear relationships. It is plausible, for example, that if MNV lesions did have a local inhibitory effect on GA growth rates, this effect would be restricted to some spatial neighborhood-of-influence surrounding the MNV (for example, due to a

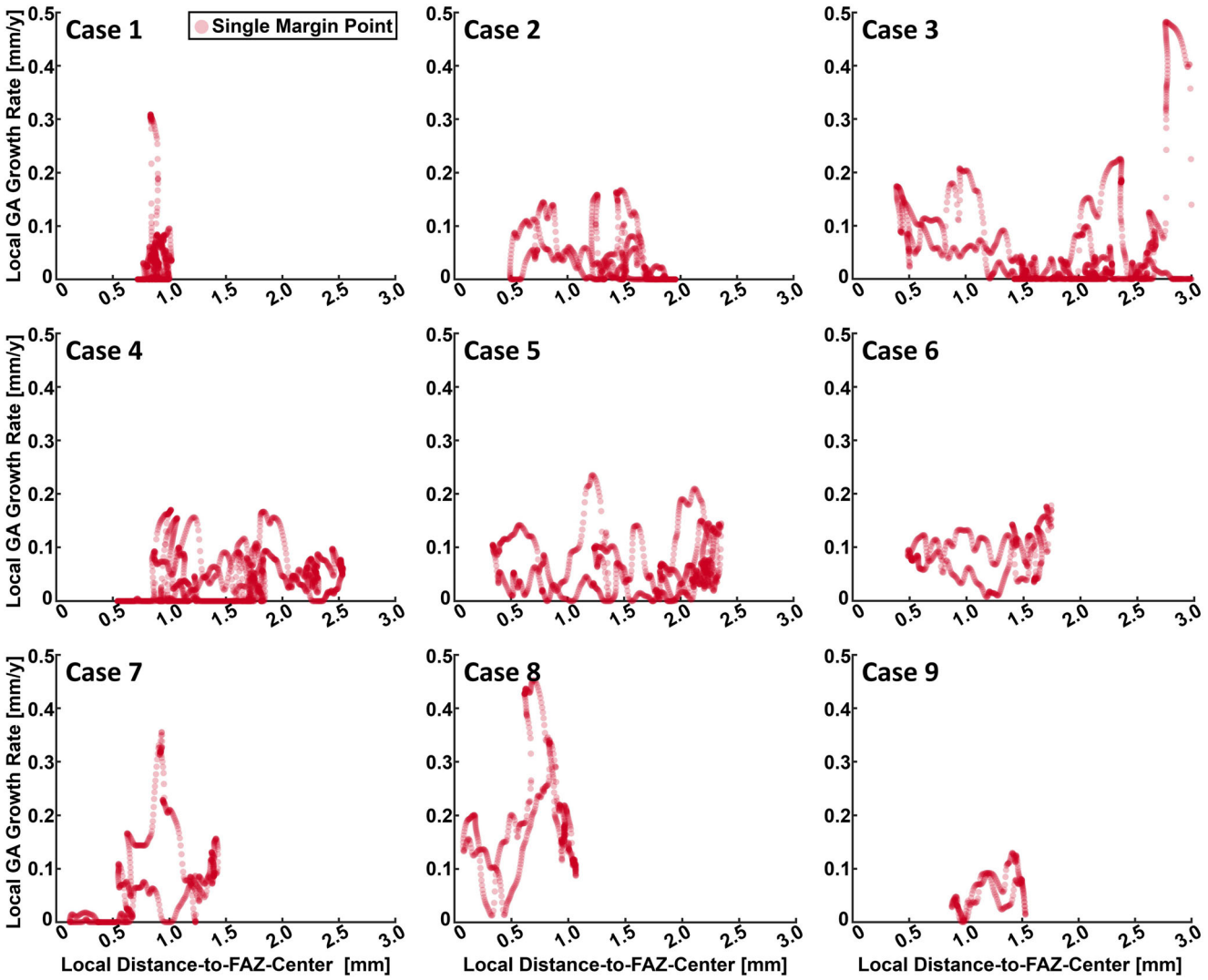

Figure 6. Scatterplots of the local geographic atrophy (GA) growth rates versus the local distance to the fovea center, estimated as the center of the foveal avascular zone as traced on the swept-source OCT angiography images divided by cases numbers.

limited diffusion distance). That is, we would not expect a margin segment located 5 mm from the MNV to grow slower than a margin segment 6 mm from the MNV due to local MNV-related inhibitory effects. Such a neighborhood effect would result in a "broken stick" or "plateauing" relationship between local GA growth rates and distances-to-MNV. This nonlinear relationship could plausibly confound a Pearson's correlation analysis when considering all margin points, which was the rationale for our 1-mm analysis. Whereas the 1 mm range is arbitrary—there are, to our knowledge, no studies examining diffusion distances from MNV lesions—a qualitative analysis of the scatter plots and bar plots gives no reason to believe that selecting a different region-of-interest (e.g. 500 µm) would have led to substantively different conclusions. Fourth, in this study, we used the MNV border tracing as a surrogate for MNV blood flow. However, MNV border tracings capture neither lesion blood flow nor capillary diffusion, which presumably would be responsible for any protective effects that might be afforded by the lesion. In particular, blood flow speed/flux[33] and vessel caliber vary both within and between MNV lesions, and these variations are not well captured by MNV border tracings. In this study, we opted to use MNV border tracings because OCTA-based quantification of blood flow speeds is still in development, and assessment of vessel morphology can be highly dependent on image quality. Nevertheless, as advances in imaging technologies continue, future studies may benefit from more nuanced measures of MNV blood flow.

Conclusion

In this study, we quantitatively assessed correlations between local GA growth rates and local distances-to-MNV using SS-OCT imaging in conjunction with GA growth modeling and spatial statistical methods. At least in the set of nine eyes examined in this study, our results do not support a local inhibitory effect on GA growth rates due to adjacent type 1 non-exudative MNV lesions.

Acknowledgments

Supported by grants from the Salah Foundation, an unrestricted grant from the Research to Prevent Blindness, Inc. (New York, NY), and the National Eye Institute Center Core Grant

Investigative Ophthalmology & Visual Science

(P30EY014801) to the Department of Ophthalmology, University of Miami Miller School of Medicine. The funding organizations had no role in the design or conduct of the present research.

This manuscript has been presented at ARVO 2021 (Virtual meeting).

Disclosure: **O. Trivizki**, None; **E.M. Moult**, VISTA-OCTA (P); **L. Wang**, None; **P. Iyer**. None; **Y. Shi**, None; **G. Gregori** receive research support from Carl Zeiss Meditec, Inc. and the University of Miami co-owns a patent that is licensed to Carl Zeiss Meditec, Inc. **W. Feuer**, None; **J.G. Fujimoto**, Optovue (I, P), Topcon (F), VISTA-OCTA (P). **P.J. Rosenfeld** also receives research support from Stealth BioTherapeutics. He is a consultant for Apellis, Biogen, Boehringer-Ingelheim, Carl Zeiss Meditec, Biogen, Chengdu Kanghong Biotech, EyePoint, Ocunexus Therapeutics, Ocudyne, and Unity Biotechnology and has equity interest in Apellis, Valitor, Verana Health, and Ocudyne

References

1. Fleckenstein M, Keenan TDL, Guymer RH, et al. Age-related macular degeneration. *Nat Rev Dis Primers.* 2021;7(1):31.
2. Sadda SR, Guymer R, Holz FG, et al. Consensus Definition for Atrophy Associated with Age-Related Macular Degeneration on OCT: Classification of Atrophy Report 3. *Ophthalmology.* 2018;125(4):537–548.
3. Spaide RF, Jaffe GJ, Sarraf D, et al. Consensus Nomenclature for Reporting Neovascular Age-Related Macular Degeneration Data: Consensus on Neovascular Age-Related Macular Degeneration Nomenclature Study Group. *Ophthalmology.* 2020;127(5):616–636.
4. Saade C, Ganti B, Marmor M, Freund KB, Smith RT. Risk characteristics of the combined geographic atrophy and choroidal neovascularisation phenotype in age-related macular degeneration. *Br J Ophthalmol.* 2014;98(12):1729–1732.
5. Schwartz SG, Agarwal A, Kovach JL, et al. The ARMS2 A69S variant and bilateral advanced age-related macular degeneration. *Retina.* 2012;32(8):1486–1491.
6. Magnusson KP, Duan S, Sigurdsson H, et al. CFH Y402H confers similar risk of soft drusen and both forms of advanced AMD. *PLoS Med.* 2006;3(1):e5.
7. Klein RJ, Zeiss C, Chew EY, et al. Complement factor H polymorphism in age-related macular degeneration. *Science.* 2005;308(5720):385–389.
8. Holz FG, Strauss EC, Schmitz-Valckenberg S, van Lookeren Campagne M. Geographic atrophy: clinical features and potential therapeutic approaches. *Ophthalmology.* 2014;121(5):1079–1091.
9. Curcio CA, Messinger JD, Sloan KR, McGwin G, Medeiros NE, Spaide RF. Subretinal drusenoid deposits in non-neovascular age-related macular degeneration: morphology, prevalence, topography, and biogenesis model. *Retina.* 2013;33(2):265–276.
10. Sarks SH. Ageing and degeneration in the macular region: a clinico-pathological study. *Br J Ophthalmol.* 1976;60(5):324–341.
11. Green WR, Key SN, 3rd. Senile macular degeneration: a histopathologic study. *Trans Am Ophthalmol Soc.* 1977;75:180–254.
12. Green WR, Enger C. Age-related macular degeneration histopathologic studies. The 1992 Lorenz E. Zimmerman Lecture. *Ophthalmology.* 1993;100(10):1519–1535.
13. Grossniklaus HE, Green WR. Choroidal neovascularization. *Am J Ophthalmol.* 2004;137(3):496–503.
14. Pfau M, Moller PT, Kunzel SH, et al. Type 1 Choroidal Neovascularization Is Associated with Reduced Localized Progression of Atrophy in Age-Related Macular Degeneration. *Ophthalmol Retina.* 2020;4(3):238–248.
15. Daniel E, Maguire MG, Grunwald JE, et al. Incidence and Progression of Nongeographic Atrophy in the Comparison of Age-Related Macular Degeneration Treatments Trials (CATT) Clinical Trial. *JAMA Ophthalmol.* 2020;138(5):510–518.
16. Gune S, Abdelfattah NS, Karamat A, et al. Spectral-Domain OCT-Based Prevalence and Progression of Macular Atrophy in the HARBOR Study for Neovascular Age-Related Macular Degeneration. *Ophthalmology.* 2020;127(4):523–532.
17. de Oliveira Dias JR, Zhang Q, Garcia JMB, et al. Natural History of Subclinical Neovascularization in Nonexudative Age-Related Macular Degeneration Using Swept-Source OCT Angiography. *Ophthalmology.* 2018;125(2):255–266.
18. Roisman L, Zhang Q, Wang RK, et al. Optical Coherence Tomography Angiography of Asymptomatic Neovascularization in Intermediate Age-Related Macular Degeneration. *Ophthalmology.* 2016;123(6):1309–1319.
19. Shen M, Zhang Q, Yang J, et al. Swept-Source OCT Angiographic Characteristics of Treatment-Naive Nonexudative Macular Neovascularization in AMD Prior to Exudation. *Invest Ophthalmol Vis Sci.* 2021;62(6):14.
20. Yang J, Zhang Q, Motulsky EH, et al. Two-Year Risk of Exudation in Eyes with Nonexudative Age-Related Macular Degeneration and Subclinical Neovascularization Detected with Swept Source Optical Coherence Tomography Angiography. *Am J Ophthalmol.* 2019;208:1–11.
21. Yehoshua Z, Wang F, Rosenfeld PJ, Penha FM, Feuer WJ, Gregori G. Natural history of drusen morphology in age-related macular degeneration using spectral domain optical coherence tomography. *Ophthalmology.* 2011;118(12):2434–2441.
22. Moult EM, Hwang Y, Shi Y, et al. Growth Modeling for Quantitative, Spatially Resolved Geographic Atrophy Lesion Kinetics. *Transl Vis Sci Technol.* 2021;10(7):26.
23. Moult EM, Shi Y, Zhang Q, et al. Analysis of correlations between local geographic atrophy growth rates and local OCT angiography-measured choriocapillaris flow deficits. *Biomed Opt Express.* 2021;12(7):4573–4595.
24. Viladomat J, Mazumder R, McInturff A, McCauley DJ, Hastie T. Assessing the significance of global and local correlations under spatial autocorrelation: a nonparametric approach. *Biometrics.* 2014;70(2):409–418.
25. Thulliez M, Zhang Q, Shi Y, et al. Correlations between Choriocapillaris Flow Deficits around Geographic Atrophy and Enlargement Rates Based on Swept-Source OCT Imaging. *Ophthalmol Retina.* 2019;3(6):478–488.
26. Yehoshua Z, Rosenfeld PJ, Gregori G, et al. Progression of geographic atrophy in age-related macular degeneration imaged with spectral domain optical coherence tomography. *Ophthalmology.* 2011;118(4):679–686.
27. Lindner M, Boker A, Mauschitz MM, et al. Directional Kinetics of Geographic Atrophy Progression in Age-Related Macular Degeneration with Foveal Sparing. *Ophthalmology.* 2015;122(7):1356–1365.
28. Mauschitz MM, Fonseca S, Chang P, et al. Topography of geographic atrophy in age-related macular degeneration. *Invest Ophthalmol Vis Sci.* 2012;53(8):4932–4939.
29. Pfau M, Lindner M, Goerdt L, et al. Prognostic Value of Shape-Descriptive Factors for the Progression of Geographic Atrophy Secondary to Age-Related Macular Degeneration. *Retina.* 2019;39(8):1527–1540.
30. Sayegh RG, Sacu S, Dunavolgyi R, et al. Geographic Atrophy and Foveal-Sparing Changes Related to Visual Acuity in

Investigative Ophthalmology & Visual Science

Patients With Dry Age-Related Macular Degeneration Over Time. *Am J Ophthalmol.* 2017;179:118–128.

31. Shen LL, Sun M, Khetpal S, Grossetta Nardini HK, Del Priore LV. Topographic Variation of the Growth Rate of Geographic Atrophy in Nonexudative Age-Related Macular Degeneration: A Systematic Review and Meta-analysis. *Invest Ophthalmol Vis Sci.* 2020;61(1):2.
32. Uji A, Nittala MG, Hariri A, Velaga SB, Sadda SR. Directional kinetics analysis of the progression of geographic atrophy. *Graefes Arch Clin Exp Ophthalmol.* 2019;257(8):1679–1685.
33. Rebhun CB, Moult EM, Ploner SB, et al. Analyzing Relative Blood Flow Speeds in Choroidal Neovascularization Using Variable Interscan Time Analysis OCT Angiography. *Ophthalmol Retina.* 2018;2(4):306–319.

Investigative Ophthalmology & Visual Science